

Dynamical transitions in scalarization and descalarization through black hole accretion

Cheng-Yong Zhang,^{1,*} Qian Chen,^{2,†} Yunqi Liu,^{3,‡} Wen-Kun Luo,^{1,§} Yu Tian,^{2,4,¶} and Bin Wang^{3,5,**}

¹Department of Physics and Siyuan Laboratory, Jinan University, Guangzhou 510632, China

²School of Physical Sciences, University of Chinese Academy of Sciences, Beijing 100049, China

³Center for Gravitation and Cosmology, College of Physical Science and Technology, Yangzhou University, Yangzhou 225009, China

⁴Institute of Theoretical Physics, Chinese Academy of Sciences, Beijing 100190, China

⁵Shanghai Frontier Science Center for Gravitational Wave Detection, Shanghai Jiao Tong University, Shanghai 200240, China

We present the first fully nonlinear study on the accretion of scalar fields onto a seed black hole in anti-de Sitter spacetime in Einstein-Maxwell-scalar theory. Intrinsic critical phenomena in the dynamical transition between the bald and scalarized black holes are disclosed. In scalarizations, the transition is discontinuous and a metastable black hole acts as an attractor at the threshold. We construct a new physical mechanism to dynamically descalarize an isolated scalarized black hole. The first results on critical phenomena in descalarizations are revealed. The dynamical descalarizations can be either discontinuous or continuous at the threshold, distinguished by whether or not an intermediate attractor appears.

Introduction. The black hole (BH) spontaneous scalarization [1–3] has received much attention recently in extended scalar-tensor-Gauss-Bonnet (eSTGB) gravity [4–6] and Einstein-Maxwell-scalar (EMS) theory [7]. Linear tachyonic instability can be triggered in bald BHs and transform them into scalarized black holes (SBHs). Moreover, the linearly stable bald BHs can also be scalarized, but through a new nonlinear mechanism, different from the spontaneous scalarization [8–11]. A fully nonlinear dynamical study showed that such scalarization can be realized through the accretion of such scalar field onto a seed BH. Novel dynamical critical behaviors at the threshold of the transition between bald and scalarized BHs were disclosed [12], which are reminiscent of the type I critical gravitational collapse [13, 14]. There exists a metastable SBH that plays the role of a critical solution separating the final scalarized and bald BHs and behaves as an attractor during the evolution.

Available studies concentrated on asymptotically flat spacetimes. It is known that dynamics in anti-de Sitter (AdS) spacetimes are different from that in asymptotically flat spacetimes. The turbulent instability in pure AdS spacetimes brings different structures in critical gravitational collapses from those in flat spaces [15–19]. Charged and rotating AdS BHs are unstable due to superradiant instability, while their counterparts are stable in asymptotically flat spacetimes [20–23]. These interesting results inspire us to further investigate novel critical phenomena in AdS spacetimes.

We explore the dynamical formation of SBHs through scalar fields accretion onto seed AdS bald BHs and examine the influence of the perturbation strength on the scalarization. We illustrate special dynamical critical phenomena in the spontaneous transition and find the bald BH playing the role of critical solution. After accretion of strong enough scalar perturbations, SBH can be descalarized. In addition to those shown in binary BH mergers [24, 25] and superradiance [26], we construct a new physical mechanism for the dynamical descalarization of an isolated SBH. We reveal the first results on the critical behaviors in dynamical descalarization. Unlike the transition at the scalarization threshold which is always

discontinuous, the transition at the descalarization threshold can be either discontinuous or continuous, depending on the specific model. Furthermore, we reveal more connections between dynamical critical scalarizations/descalarizations and critical gravitational collapses in [17–19].

Numerical setup. The action of the EMS theory in AdS spacetime is

$$S = \int d^4x \sqrt{-g} (R + \frac{6}{L^2} - 2\nabla_\mu \phi \nabla^\mu \phi - f(\phi) F_{\mu\nu} F^{\mu\nu}), \quad (1)$$

where R is the Ricci scalar and L is the AdS radius. The real scalar field ϕ couples to the Maxwell field $F_{\mu\nu} \equiv \partial_\mu A_\nu - \partial_\nu A_\mu$ through function $f(\phi)$. We consider a model with $f = e^{\alpha\phi^2}$, which can trigger the linear tachyonic instability in Reissner-Nordström (RN) AdS BHs with large charge to mass ratio, so that the spontaneous scalarization occurs and the stable solutions become SBHs [27, 28]. Further we consider a model with $f = e^{\beta\phi^4}$ and show that the RN-AdS BH is linearly stable against small perturbation, but nonlinearly unstable against large perturbation and evolves into a SBH in AdS spacetime through a new nonlinear mechanism beyond the spontaneous scalarization. Here α, β are coupling constants.

To study the nonlinear BH dynamics in spherically symmetric asymptotically AdS spacetime, we take the ingoing Eddington-Finkelstein coordinate [29]:

$$ds^2 = -W dt^2 + 2dt dr + \Sigma^2 (d\theta^2 + \sin^2 \theta d\varphi^2). \quad (2)$$

Here W, Σ are metric functions of (t, r) . This coordinate is regular on the BH apparent horizon r_h satisfying $g^{\mu\nu} \partial_\mu \Sigma \partial_\nu \Sigma = 0$ which implies the vanishing of auxiliary variable $S \equiv \partial_t \Sigma + \frac{1}{2} W \partial_r \Sigma$. The BH irreducible mass $M_h(t) \equiv \sqrt{\frac{V_h}{4\pi}} = \Sigma(r_h, t)$ where V_h is the apparent horizon area. It measures the thermodynamic entropy of a BH. We take the gauge field $A_\mu dx^\mu = A(t, r) dt$. The Maxwell equation gives $\partial_r A = \frac{Q}{\Sigma^2 f}$. Here Q is the BH charge. Introducing auxiliary variable

$$P = \partial_t \phi + \frac{1}{2} W \partial_r \phi, \quad (3)$$

the Einstein equations give

$$\partial_r^2 \Sigma = -\Sigma(\partial_r \phi)^2, \quad (4)$$

$$\partial_r S = \frac{1 - 2S\partial_r \Sigma}{2\Sigma} + \frac{3\Sigma}{2L^2} - \frac{Q^2}{2\Sigma^3 f}, \quad (5)$$

$$\partial_r^2 W = -4P\partial_r \phi + \frac{4S\partial_r \Sigma - 2}{\Sigma^2} + \frac{4Q^2}{\Sigma^4 f}, \quad (6)$$

$$\partial_t S = \frac{S\partial_r W - W\partial_r S}{2} - \Sigma P^2. \quad (7)$$

The scalar equation gives

$$\partial_r P = -\frac{P\partial_r \Sigma + S\partial_r \phi}{\Sigma} - \frac{Q^2}{4\Sigma^4 f^2} \frac{df}{d\phi}. \quad (8)$$

The asymptotic behaviors of the variables are

$$\phi = \frac{\phi_3(t)}{r^3} + O(r^{-4}), \quad (9)$$

$$\Sigma = r + \lambda(t) - \frac{3\phi_3(t)^2}{10r^5} + O(r^{-6}), \quad (10)$$

$$S = \frac{(r + \lambda(t))^2}{2L^2} + \frac{1}{2} - \frac{M}{r} + O(r^{-2}), \quad (11)$$

$$P = -\frac{3\phi_3(t)}{2L^2 r^2} + O(r^{-3}), \quad (12)$$

$$W = \frac{(r + \lambda(t))^2}{L^2} - 2\dot{\lambda}(t) + 1 - \frac{2M}{r} + O(r^{-2}), \quad (13)$$

Here the constant M represents the ADM mass. $\phi_3(t)$ is an unknown function of time that is determined by the dynamics. $\lambda(t)$ is a residual gauge freedom [21, 29] and the dot denotes the time derivative. The procedure to solve these equations, the boundary conditions and the test of the convergence are shown in the supplement material.

Hereafter we fix $L = 1$ such that all physical quantities are measured by the AdS radius. Without loss of generality, we choose the initial configuration as a seed RN-AdS BH with $M_0 = 1, Q = 0.8$ and simulate the evolution under initial scalar data $\phi_0 = pe^{-64(0.5 - \frac{1}{r})^2}$. The dynamical critical behaviors for both scalarization and descalarization are not changed qualitatively for different parameters and initial scalar data families. The ADM mass M increases with p such that the evolution of the system can be viewed as the accretion of scalar field onto the central BH.

For any initial data and coupling functions, we find universal and robust relations during the evolution,

$$\ln \dot{M}_h = 2 \ln |\dot{\phi}_h| + \text{const}. \quad (14)$$

Here $\phi_h(t)$ is the scalar value on the apparent horizon. M_h never decreases in evolution due to the second law of black hole mechanics. These relations can be partially understood from the perturbative analysis for stationary solutions, in which $S, W, P|_{r_h} = 0$ on the horizon. Combining (5,7,8), there are $\partial_t S, \partial_t \Sigma|_{r_h} \propto \delta\phi^2$. Since $M_h = \Sigma(r_h, t)$ and r_h satisfies $S(r_h, t) = 0$, we have $\dot{M}_h = -\frac{\partial_r S}{\partial_r \Sigma} \partial_r \Sigma|_{r_h} + \partial_t \Sigma|_{r_h} \propto \dot{\phi}_h^2$. Thus (14) is expected for a solution which

can be approximated by a stationary solution. However, (14) holds even in the highly nonlinear regime and calls for further exploration [12, 28, 30–32].

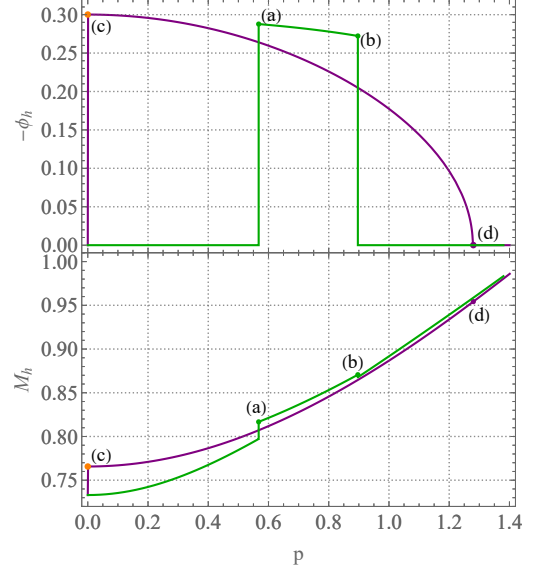


FIG. 1. The final values of ϕ_h and M_h versus p of initial data $\phi_0 = pe^{-64(0.5 - \frac{1}{r})^2}$. The green and purple lines are results for $f(\phi) = e^{500\phi^4}, e^{15\phi^2}$ respectively. The system begins to undergo the process of scalarization and descalarization at the critical points ($p_a = 0.56736843744772 \pm 10^{-14}, p_c = 0$) and ($p_b = 0.89673160782993 \pm 10^{-14}, p_d = 1.2784440 \pm 10^{-7}$), respectively. Note that the system needs very long time to reach equilibrium near p_d , so it is more expensive to calculate until the high accuracy 10^{-14} . Moreover, the critical behavior has shown up when we reach the accuracy 10^{-7} and will not change if we further improve the accuracy.

Numerical results for scalarization. We show the final values of M_h and ϕ_h with respect to parameter p when the system reaches equilibrium after the initial perturbation in Fig.1. For a model with $f = e^{15\phi^2}$, both ϕ_h and M_h jump at threshold $p_c = 0$. The nonzero final ϕ_h marks the formation of a SBH. The initial RN-AdS BH is spontaneously scalarized due to the tachyonic instability. For a model with $f = e^{500\phi^4}$, the initial RN-AdS BH is linearly stable and all small perturbations are absorbed, resulting a larger scalar-free RN-AdS BH. But it becomes nonlinearly unstable when p is larger than the threshold p_a , where both ϕ_h and M_h jump. The nonlinear instability indicates a new mechanism for the AdS BH scalarization that is different from the spontaneous scalarization [28]. This is reflected in the different scaling of ϕ_h for SBHs near thresholds $p_{a,c}$, as shown in Fig.2,

$$|\phi_h - \phi_i| \propto |p - p_i|^{\gamma_i}. \quad (15)$$

Here subscript $i \in a, c$ and ϕ_i is the final ϕ_h for threshold p_i . The exponent $\gamma_{a,c} = 1, 2$ are independent of the initial scalar data family, the BH parameters and the coupling parameters α, β . However, the nontrivial power law for the BH irreducible mass like in asymptotically flat spacetime [12]

is absent here, due to the confining AdS boundary which prohibits energy escape.

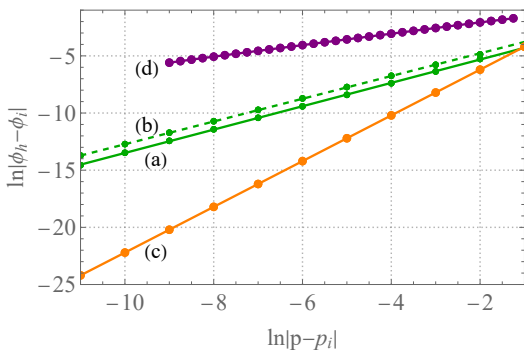


FIG. 2. The final ϕ_h of SBHs versus p near the thresholds. The solid/dashed green, orange and purple lines are for those near $p_{a,b,c,d}$ in Fig.1, respectively.

In Fig.3(a) we display the evolution of ϕ_h , M_h and $\ln|\dot{\phi}_h|$ for the model with $f = e^{500\phi^4}$ near threshold p_a . All solutions are attracted to an intermediate plateau corresponding to a critical solution (CS), which is a metastable SBH behaving as an attractor. At late times, the solutions decay to bald AdS BHs if $p < p_a$, or to SBHs if $p > p_a$. The evolution can be divided into three stages, as refined in the bottom of Fig.3(a). At the first stage, the solutions converge to the CS with the dominant mode frequency $\omega_a^c = 2.81 - 1.61i$, where the superscript c denotes the CS. At the second stage, the solutions depart the CS with $|\dot{\phi}_h| \propto e^{\eta_a t}$ in which $\eta_a = 0.861$. The time T_a of the intermediate solutions (the first and second stages) stay near the plateau scales as

$$T_a = -\eta_a^{-1} \ln|p - p_a| + \text{const}, \quad (16)$$

as shown in Fig.4. Based on these observations, we conclude

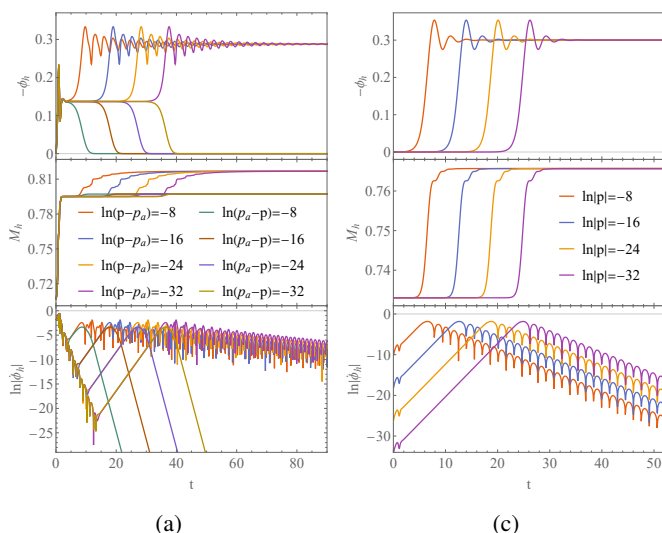


FIG. 3. The evolution of the M_h , ϕ_h , and $\ln|\dot{\phi}_h|$ near the thresholds p_a (left) and p_c (right).

that the intermediate solutions $\phi_p(t, r)$ near the threshold p_a can be approximated by

$$\phi_p(t, r) \approx \phi_a(r) + (p - p_a)e^{\eta_a t} \delta\phi_a(r) + \text{stable modes}. \quad (17)$$

Here $\delta\phi_a(r)$ is the unstable eigenmode with eigenvalue η_a for the CS $\phi_a(r)$. The unstable mode grows to a finite size in time T_a , after which the solutions converge either to larger bald RN-AdS BHs with dominant mode $\omega_a^b = -2.33i$ if $p < p_a$, or to SBHs with dominant mode $\omega_a^s = 2.31 - 0.0649i$ if $p > p_a$. Superscripts b, s denote bald, scalarized BHs respectively.

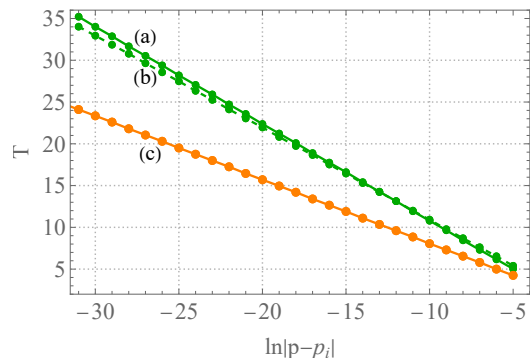


FIG. 4. The time T of the intermediate solutions staying near the CSs versus $\ln|p - p_i|$. The solid, dashed green and orange lines are for thresholds $p_{a,b,c}$, respectively.

In Fig.3(c) we show the evolution of ϕ_h , M_h and $\ln|\dot{\phi}_h|$ for the model with $f = e^{15\phi^2}$ near threshold p_c . They look qualitatively similar to those in Fig.3(a), except some intriguing differences. Here only SBH survives as the final state and the initial RN-AdS BH plays the role of a CS. The intermediate solution stays near it with time $T_c \propto -\eta_c^{-1} \ln|p|$ where $\eta_c = 1.31$, as shown in Fig.4. The evolution here is actually a special case of (17) with threshold $p_c = 0$ and CS $\phi_c(r) = 0$. After T_c , the solution converges to the final SBH with dominant mode $\omega_c^s = 2.06 - 0.524i$.

Numerical results for descalarization. The dynamical descalarization induced by binary BH mergers in eSTGB theory [24, 25] and superradiance in EMS theory [26] has been reported. Here we show that when the energy of the initial perturbation is large enough, the accretion of scalar field onto an isolated SBH can also trigger the scalar field dissipation and descalarize the SBH. As shown in Fig.1, we observe that ϕ_h gradually or suddenly drops to zero at thresholds $p_{d,b}$ for models with $f = e^{15\phi^2}, e^{500\phi^4}$, respectively. These indicate two kinds of phenomena in the dynamical descalarization through accretion, which are continuous or discontinuous at thresholds $p_{d,b}$, respectively. The scaling law (15) still hold here, but with universal exponents $\gamma_{d,b} = 1, 0.5$ respectively. The reason for this significant difference in the dynamic processes is the different phase structures possessed by the two models. This will be described from the perspective of static solutions in the next section.

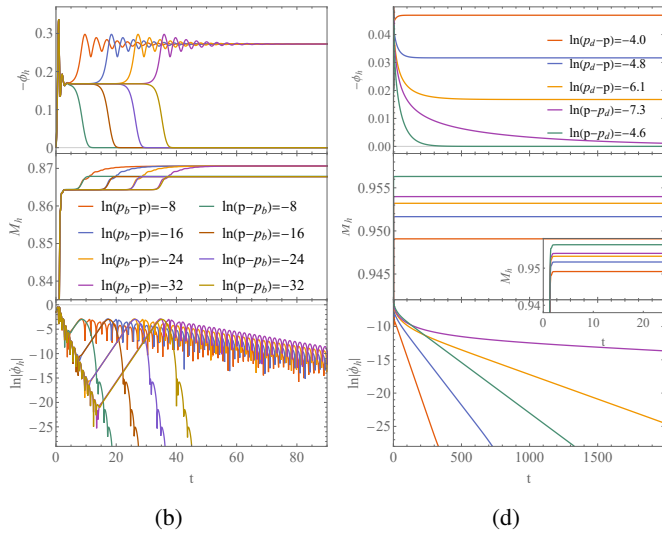


FIG. 5. The evolution of the M_h , ϕ_h , and $\ln|\dot{\phi}_h|$ near the thresholds p_b (left) and p_d (right).

As shown in Fig.5(b), the evolution near the descalarization threshold p_b is qualitatively the same with that near the scalarization threshold p_a . The intermediate solutions are attracted to a CS with dominant mode $\omega_b^c = 3.25 - 1.55i$. Then the solutions depart the CS with $|\dot{\phi}_h| \propto e^{\eta_b t}$ where $\eta_b = 0.906$. The time T_b of the intermediate solution that stays near the CS scales as $T_b \propto -\eta_b^{-1} \ln|p - p_b|$, as exhibited in Fig.4. After T_b , the solution keeps scalarized with dominant mode $\omega_b^s = 1.88 - 0.104i$ if $p < p_b$, or decays to a bald BH with dominant mode $\omega_b^b = 2.21 - 3.01i$ if $p > p_b$.

The critical phenomena of the descalarization near threshold p_d are special, as shown in Fig.5(d). There is no attractor at the threshold. Given p , we find that the scalar field exponentially decays at late times with the same rate in the whole space. However, for different p , the late time exponential decay rate varies with p as $\omega_d^s = (3.20p - 4.09)i$ for the final SBH when $p < p_d$, or $\omega_d^b = (2.01 - 1.57p)i$ for the final bald RN-AdS BH when $p > p_d$. Both ω_d^s and ω_d^b are zero at threshold p_d . This is also qualitatively different from those near $p_{a,b,c}$ which are independent of p .

Static solutions and thermodynamics. In Fig.6 we illustrate the BH irreducible mass versus the ADM mass for the two branches of static solutions: the RN-AdS BHs and SBHs. For the model with $f = e^{15\phi^2}$ shown in the inset, the static SBH smoothly intersects the static RN-AdS BH at point (d). Before point (d), the RN-AdS BH is unstable under arbitrarily small perturbation and dynamically evolves to the SBH which is also favored by thermodynamics. After point (d), only the static RN-AdS BH solutions survives and it becomes stable under small perturbation. The final state of the dynamical evolution turns from the SBH to the RN-AdS BH at point (d). Combining with Fig.1 we see that here the descalarization is a continuous phase transition. For the model with $f = e^{500\phi^4}$, the RN-AdS and the SBHs coexist before point (e). But now they both are linearly stable. So

although the SBH has larger or smaller entropy than the RN-AdS BH before or after point (x), a small perturbation does not necessarily lead to a dynamical transition between the two branches of stable solutions. However, with a sufficiently large quench, the system can be interconverted between these two stable states. The dynamic process is a first-order phase transition and does not generically coincide with the equilibrium thermodynamic preference for static solutions.

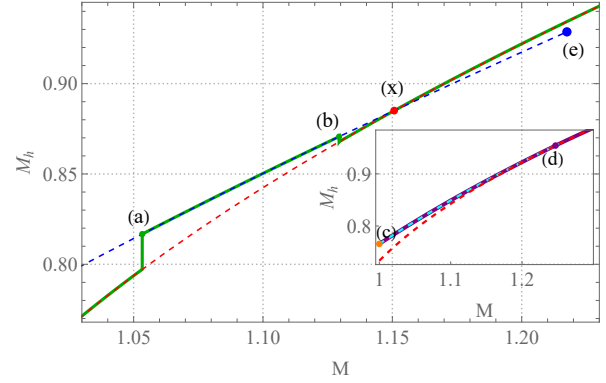


FIG. 6. The black hole irreducible mass versus the ADM mass for static solutions. The dashed red lines are for the static RN-AdS solutions. The dashed blue and cyan (inset) lines for the static SBH solutions in models with $f = e^{500\phi^4}$, $e^{15\phi^2}$, respectively. The intersection points (x)=(1.1507, 0.8851) and (d)=(1.2469, 0.9542). There are no static SBHs beyond (e)=(1.2175, 0.9287) for $f = e^{500\phi^4}$, or (d) for $f = e^{15\phi^2}$. The solid green and purple lines correspond to those in Fig.1 obtained in nonlinear evolution.

Summary and discussion. We have studied for the first time the scalarization in AdS spacetime through nonlinear accretion of scalar field onto a central BH. In the dynamical spontaneous scalarization, the RN-AdS BH plays the role of a CS and only SBH survives as the final state. For a new nonlinear mechanism beyond the spontaneous scalarization, we revealed that a linearly stable bald BH can be transformed into a SBH, provided that the perturbation strength is over a threshold. Near the threshold, a metastable SBH in AdS spacetime acts as an attractor separating the final bald and scalarized BHs. The transitions at the scalarization thresholds in both cases are of the first order resembling the type I critical collapse [13, 14]. However, due to the confining AdS boundary, the final BH mass does not follow a nontrivial power-law as found in asymptotically flat spacetime [12].

We have constructed a new physical mechanism for the dynamical descalarization of an isolated SBH through accretion of scalar field. For a model with $f = e^{\alpha\phi^2}$, the final BH mass and scalar field changes continuously with a nontrivial universal power-law at the descalarization threshold, resembling the type II critical collapse [17–19]. No attractor appears during the dynamical descalarization. For $f = e^{\beta\phi^4}$, we observe sudden drops in both the final scalar field and BH irreducible mass at the descalarization threshold, indicating a first order transition. There is an attractor separating the final scalarized and bald BHs in such transition resembling the type I critical collapse.

The dynamical critical behaviors we disclosed in this work are not limited in the EMS theory. The first-order strong gravity phase transitions exist in other physical models, such as the eSTGB theory [10, 11], the BH with Q-cloud [33, 34], black ring [35, 36], holographic models such as the holographic QCD etc [37–39]. They also resemble the first-order matter phase transition in neutron star binary mergers [40, 41]. It is expected that the study of dynamical critical behaviors in our work can shed lights into deep investigations of dynamical mechanisms in many alternative gravity models. Uncovering these mechanisms can provide better understanding on the gravitational wave emission.

Acknowledgments. This research is supported by National Key R&D Program of China under Grant No.2020YFC2201400, and the Natural Science Foundation of China under Grant Nos. 11975235, 12005077, 12035016 and Guangdong Basic and Applied Basic Research Foundation under Grant No. 2021A1515012374. B. W. was partially supported by NNSFC under grant 12075202.

* zhangcy@email.jnu.edu.cn

† chenqian192@mails.ucas.ac.cn (corresponding author)

‡ yunqiliu@yzu.edu.cn

§ luowk@stu2020.jnu.edu.cn

¶ ytian@ucas.ac.cn

** wang_b@sju.edu.cn (corresponding author)

- [1] T. Damour and G. Esposito-Farese, Nonperturbative strong field effects in tensor-scalar theories of gravitation, *Phys. Rev. Lett.*, vol. 70, pp. 2220-2223,
- [2] T. Damour and G. Esposito-Farese, “Tensor-scalar gravity and binary pulsar experiments,” *Phys. Rev. D* 54 (1996), 1474-1491 [arXiv:gr-qc/9602056 [gr-qc]].
- [3] T. Harada, “Stability analysis of spherically symmetric star in scalar-tensor theories of gravity,” *Prog. Theor. Phys.* 98 (1997), 359-379 [arXiv:gr-qc/9706014 [gr-qc]].
- [4] D. D. Doneva and S. S. Yazadjiev, New Gauss-Bonnet Black Holes with Curvature-Induced Scalarization in Extended Scalar-Tensor Theories, *Phys. Rev. Lett.* 120, no.13, 131103 (2018) [arXiv:1711.01187 [gr-qc]].
- [5] H. O. Silva, J. Sakstein, L. Gualtieri, T. P. Sotiriou and E. Berti, Spontaneous scalarization of black holes and compact stars from a Gauss-Bonnet coupling, *Phys. Rev. Lett.* 120, no.13, 131104 (2018) [arXiv:1711.02080 [gr-qc]].
- [6] G. Antoniou, A. Bakopoulos and P. Kanti, Evasion of No-Hair Theorems and Novel Black-Hole Solutions in Gauss-Bonnet Theories, *Phys. Rev. Lett.* 120, no.13, 131102 (2018) [arXiv:1711.03390 [hep-th]].
- [7] C. A. R. Herdeiro, E. Radu, N. Sanchis-Gual and J. A. Font, “Spontaneous Scalarization of Charged Black Holes,” *Phys. Rev. Lett.* 121, no. 10, 101102 (2018). [arXiv:1806.05190].
- [8] J. L. Blázquez-Salcedo, C. A. R. Herdeiro, J. Kunz, A. M. Pombo and E. Radu, “Einstein-Maxwell-scalar black holes: the hot, the cold and the bald,” *Phys. Lett. B* 806, 135493 (2020) [arXiv:2002.00963 [gr-qc]].
- [9] J. L. Blázquez-Salcedo, S. Kahlen and J. Kunz, “Critical solutions of scalarized black holes,” *Symmetry* 12, no.12, 2057 (2020) [arXiv:2011.01326 [gr-qc]].
- [10] D. D. Doneva and S. S. Yazadjiev, “Beyond the spontaneous scalarization: New fully nonlinear mechanism for the formation of scalarized black holes and its dynamical development,” *Phys. Rev. D* 105, no.4, L041502 (2022) [arXiv:2107.01738 [gr-qc]].
- [11] Y. Liu, C. Y. Zhang, Q. Chen, Z. Cao, Y. Tian and B. Wang, “The critical scalarization and descalarization of black holes in a generalized scalar-tensor theory,” [arXiv:2208.07548 [gr-qc]].
- [12] C. Y. Zhang, Q. Chen, Y. Liu, W. K. Luo, Y. Tian and B. Wang, “Critical phenomena in dynamical scalarization of charged black hole,” [arXiv:2112.07455 [gr-qc]].
- [13] P. Bizon and T. Chmaj, “Critical collapse of Skyrmions,” *Phys. Rev. D* 58 (1998), 041501 [arXiv:gr-qc/9801012 [gr-qc]].
- [14] M. W. Choptuik, T. Chmaj and P. Bizon, “Critical behavior in gravitational collapse of a Yang-Mills field,” *Phys. Rev. Lett.* 77 (1996), 424-427 [arXiv:gr-qc/9603051 [gr-qc]].
- [15] P. Bizon and A. Rostworowski, “On weakly turbulent instability of anti-de Sitter space,” *Phys. Rev. Lett.* 107 (2011), 031102 [arXiv:1104.3702 [gr-qc]].
- [16] M. W. Choptuik, “Universality and scaling in gravitational collapse of a massless scalar field,” *Phys. Rev. Lett.* 70 (1993), 9-12
- [17] S. L. Liebling and M. W. Choptuik, “Black hole criticality in the Brans-Dicke model,” *Phys. Rev. Lett.* 77, 1424-1427 (1996) [arXiv:gr-qc/9606057 [gr-qc]].
- [18] C. R. Evans and J. S. Coleman, “Observation of critical phenomena and selfsimilarity in the gravitational collapse of radiation fluid,” *Phys. Rev. Lett.* 72, 1782-1785 (1994).
- [19] C. Gundlach and J. M. Martin-Garcia, “Critical phenomena in gravitational collapse,” *Living Rev. Rel.* 10 (2007), 5 [arXiv:0711.4620 [gr-qc]].
- [20] P. Bosch, S. R. Green and L. Lehner, “Nonlinear Evolution and Final Fate of Charged Anti-de Sitter Black Hole Superradiant Instability,” *Phys. Rev. Lett.* 116, no.14, 141102 (2016) [arXiv:1601.01384 [gr-qc]].
- [21] P. M. Chesler and D. A. Lowe, “Nonlinear Evolution of the AdS₄ Superradiant Instability,” *Phys. Rev. Lett.* 122, no.18, 181101 (2019) [arXiv:1801.09711 [gr-qc]].
- [22] E. Berti, V. Cardoso and A. O. Starinets, “Quasinormal modes of black holes and black branes,” *Class. Quant. Grav.* 26, 163001 (2009) [arXiv:0905.2975 [gr-qc]].
- [23] R. Brito, V. Cardoso and P. Pani, “Superradiance: New Frontiers in Black Hole Physics,” *Lect. Notes Phys.* 906, pp.1-237 (2015) [arXiv:1501.06570 [gr-qc]].
- [24] H. O. Silva, H. Witek, M. Elley and N. Yunes, “Dynamical Descalarization in Binary Black Hole Mergers,” *Phys. Rev. Lett.* 127, no.3, 031101 (2021) [arXiv:2012.10436 [gr-qc]].
- [25] D. D. Doneva, A. Vañó-Viñuales and S. S. Yazadjiev, “Dynamical descalarization with a jump during black hole merger,” [arXiv:2204.05333 [gr-qc]].
- [26] F. Corelli, T. Ikeda and P. Pani, “Challenging cosmic censorship in Einstein-Maxwell-scalar theory with numerically simulated gedanken experiments,” *Phys. Rev. D* 104, no.8, 084069 (2021) [arXiv:2108.08328 [gr-qc]].
- [27] G. Guo, P. Wang, H. Wu and H. Yang, “Scalarized Einstein-Maxwell-scalar black holes in anti-de Sitter spacetime,” *Eur. Phys. J. C* 81, no.10, 864 (2021) [arXiv:2102.04015 [gr-qc]].
- [28] C. Y. Zhang, P. Liu, Y. Liu, C. Niu and B. Wang, “Dynamical charged black hole spontaneous scalarization in anti-de Sitter spacetimes,” *Phys. Rev. D* 104 (2021) no.8, 084089 [arXiv:2103.13599 [gr-qc]].
- [29] P. M. Chesler and L. G. Yaffe, “Numerical solution of gravitational dynamics in asymptotically anti-de Sitter spacetimes,” *JHEP* 07, 086 (2014) [arXiv:1309.1439 [hep-th]].
- [30] C. Y. Zhang, P. Liu, Y. Liu, C. Niu and B. Wang, “Dynamical

- scalarization in Einstein-Maxwell-dilaton theory,” Phys. Rev. D **105**, no.2, 024073 (2022) [arXiv:2111.10744 [gr-qc]].
- [31] C. Y. Zhang, P. Liu, Y. Liu, C. Niu and B. Wang, “Evolution of anti-de Sitter black holes in Einstein-Maxwell-dilaton theory,” Phys. Rev. D **105**, no.2, 024010 (2022) [arXiv:2104.07281].
- [32] W. K. Luo, C. Y. Zhang, P. Liu, C. Niu and B. Wang, “Dynamical spontaneous scalarization in Einstein-Maxwell-scalar models in anti-de Sitter spacetime,” [arXiv:2206.05690 [gr-qc]].
- [33] C. A. R. Herdeiro and E. Radu, “Spherical electro-vacuum black holes with resonant, scalar Q -hair,” Eur. Phys. J. C **80**, no.5, 390 (2020) [arXiv:2004.00336 [gr-qc]].
- [34] J. P. Hong, M. Suzuki and M. Yamada, “Spherically Symmetric Scalar Hair for Charged Black Holes,” Phys. Rev. Lett. **125**, no.11, 111104 (2020) [arXiv:2004.03148 [gr-qc]].
- [35] R. Emparan and H. S. Reall, “A Rotating black ring solution in five-dimensions,” Phys. Rev. Lett. **88**, 101101 (2002) [arXiv:hep-th/0110260 [hep-th]].
- [36] R. Emparan, T. Harmark, V. Niarchos, N. A. Obers and M. J. Rodriguez, “The Phase Structure of Higher-Dimensional Black Rings and Black Holes,” JHEP **10**, 110 (2007) [arXiv:0708.2181 [hep-th]].
- [37] S. S. Gubser and A. Nellore, “Mimicking the QCD equation of state with a dual black hole,” Phys. Rev. D **78**, 086007 (2008) [arXiv:0804.0434 [hep-th]].
- [38] R. A. Janik, J. Jankowski and H. Soltanpanahi, “Real-Time dynamics and phase separation in a holographic first order phase transition,” Phys. Rev. Lett. **119**, no.26, 261601 (2017) [arXiv:1704.05387 [hep-th]].
- [39] M. Attems, Y. Bea, J. Casallerrey-Solana, D. Mateos and M. Zilhão, “Dynamics of Phase Separation from Holography,” JHEP **01**, 106 (2020) [arXiv:1905.12544 [hep-th]].
- [40] E. R. Most, L. J. Papenfort, V. Dexheimer, M. Hanauske, S. Schramm, H. Stöcker and L. Rezzolla, “Signatures of quark-hadron phase transitions in general-relativistic neutron-star mergers,” Phys. Rev. Lett. **122**, no.6, 061101 (2019) [arXiv:1807.03684 [astro-ph.HE]].
- [41] S. Zha, E. P. O’Connor, M. c. Chu, L. M. Lin and S. M. Couch, “Gravitational-Wave Signature of a First-Order Quantum Chromodynamics Phase Transition in Core-Collapse Supernovae,” Phys. Rev. Lett. **125**, no.5, 051102 (2020) [arXiv:2007.04716 [astro-ph.HE]].

SUPPLEMENT MATERIAL

Besides those presented in the main text, we actually did many calculations with different initial values of M_0, Q and the parameters α, β in coupling functions $f = e^{\alpha\phi^2}$ or $e^{\beta\phi^4}$. We found that only for large α, β and Q/M_0 , the initial RN-AdS black hole can be scalarized. But the dynamical critical behaviors for both scalarization and descalarization are not changed qualitatively for different parameters and initial scalar data families. Thus our results reported in the main text are sound.

Now we explain in details about our numerical method, boundary conditions and our test of convergence. We follow an efficient integration strategy [29] suitable for our works.

Given ϕ , equation (4) is a linear second order radial ordinary differential equation (ODE) for Σ . The two integration constants are fixed by the first and second terms

in the asymptotic behavior (10): $\Sigma \sim r + \lambda$. Here the initial gauge λ is determined by the radial position of the initial apparent horizon. For example, if the initial configuration is a RN-AdS BH with $S(r') = \frac{r'^2}{2L^2} + \frac{1}{2} - \frac{M}{r'} + \frac{Q^2}{2r'^2}$, then the initial λ is determined by shifting the radius of horizon r'_h to the boundary of computing domain $r_h = r'_h - \lambda = 1$.

Once ϕ and Σ are known, equation (5) can be integrated to solve S . In our simulation, the apparent horizon condition $S(r_h) = 0$ is used to fix the single integration constant in (5) (Another option is to use the ADM mass M as the integration constant. We do not adopt this option here).

For equation (8), the single needed integration constant can be fixed by the coefficient of the leading term in (12): $P \sim -\frac{3\phi_3}{2L^2r^2}$, where ϕ_3 can be extracted from the asymptotic behavior of the already known scalar field (9).

Equation (6) is a linear second order ODE for W , whose source term depends only on the solved variables (ϕ, Σ, S, P). We choose the gauge so that the position of the apparent horizon is time invariant, which implies $\partial_t S|_{r_h} = 0$ and gives a boundary condition for W at the horizon from (7):

$$W(r_h) = -\left. \frac{2\Sigma P^2}{\partial_r S} \right|_{r_h}. \quad (18)$$

Besides the boundary condition (18) fixing one of the two integration constants, another integration constant is fixed by the leading term in the asymptotic behavior (13), $W \sim r^2/L^2$.

Once W is determined, one can extract the time derivatives of scalar field ϕ and shift λ from the auxiliary variable P (3) and the asymptotic behavior of W (13), respectively.

$$\partial_t \phi = P - \frac{1}{2} W \partial_r \phi, \quad (19)$$

$$\partial_t \lambda = -\frac{1}{2} \lim_{r \rightarrow \infty} \left[W - \frac{(r + \lambda)^2}{L^2} - 1 \right]. \quad (20)$$

Then one can push the scalar field ϕ and shift λ to the next time slice by integrating in time for (19, 20). The procedure is iterated until the entire simulation is completed.

To improve the stability and accuracy, we introduce new variables g, σ, s, p, a in the numerical code as follows.

$$\phi \equiv \frac{g}{r^3}, \Sigma \equiv r + \lambda + \frac{1}{r^3} \sigma, \quad (21)$$

$$S \equiv \frac{(r + \lambda)^2}{2L^2} + \frac{1}{2} + \frac{1}{r} s, \quad (22)$$

$$P \equiv -\frac{3\phi_3}{2L^2r^2} + \frac{1}{r^3} p, \quad (23)$$

$$W \equiv \frac{(r + \lambda)^2}{L^2} + 1 + a. \quad (24)$$

The boundary conditions should be reorganized to apply to g, σ, s, p, a . We compactify the radial coordinate by $z = 1/r$ such that $z = 1$ corresponds to the apparent horizon and $z = 0$ to the AdS boundary. The new radial coordinate z is discretized with N Chebyshev–Gauss–Lobatto points $z_m = \frac{1}{2}(1 + \cos \frac{n\pi}{N})$ for $n = 0, 1, \dots, N$. The constraint equations

(4-8) are solved with collocation approach. The evolution equations (19, 20) are solved with classic fourth order Runge-Kutta method.

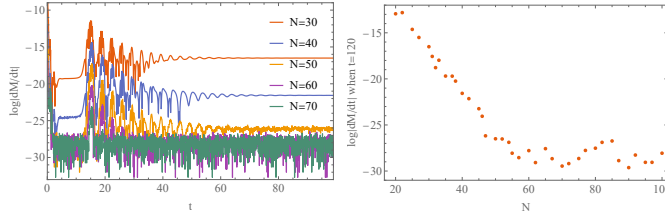


FIG. 7. The accuracy and convergence of our numerical code. Left: the evolution of $\log|\partial_t M|$ with different grid points N . Right: the value of $\log|\partial_t M|$ when $t = 120$ for different N . Here we show the results of the evolution starting with a RN-AdS black hole with $M_0 = 1, Q = 0.8$ in the EMS model with $f = e^{500\phi^4}$ under perturbation $\phi_0 = pe^{-64(0.5 - \frac{1}{r})^2}$ with $p = 0.89673$.

The redundant equation (7) allows us to detect the numerical errors during the evolution (it reduces to (18) at the apparent horizon and gives one boundary condition for W). Without loss of generality, we use the asymptotic behavior of equation (7) at the AdS boundary, which generates the energy conservation condition $\partial_t M = 0$, to show the numerical error. Fig.7 shows that the accuracy of our code improves exponentially as the grid points increase when $N \lesssim 60$. All results shown in the paper are obtained with $N = 100$.